Hybrid Optimization for 3D Landmark Extraction:Genetic Algorithms and Conjugate Gradient Method

Manfred Alker[1], Sönke Frantz[1], Karl Rohr[2], and H. Siegfried Stiehl[1]

[1] Universität Hamburg, FB Informatik, AB Kognitive Systeme, Vogt-Kölln-Str. 30, D-22527 Hamburg, Email: {alker,frantz,stiehl}@kogs.informatik.uni-hamburg.de
[2] International University in Germany, D-76646 Bruchsal, Email: rohr@i-u.de

Zusammenfassung. Model fitting algorithms for the extraction of 3D point landmarks tend to run into local suboptima if the model parameters are poorly initialized. We therefore propose a generally applicable *novel hybrid optimization algorithm* that combines the time efficiency of conjugate gradient (cg-)optimization and the robustness of genetic algorithms against local suboptima. We apply our algorithm to 3D MR and CT images depicting tip-like and saddle-like anatomical structures in order to demonstrate that the robustness of model fitting is significantly improved in comparison to purely local cg-optimization.

1 Introduction

The extraction of 3D point landmarks is a prerequisite for point landmark-based 3D image registration. While earlier approaches are based on differential operators ([4]), an approach based on fitting deformable models to the image data by minimizing a fitting measure has recently been proposed in [3]. However, since local optimization is used in [3], a good model initialization is needed. To overcome this drawback, we propose a hybrid optimization algorithm which is a combination of a purely local conjugate gradient method and a genetic algorithm. Exemplarily, we apply our fitting algorithm to the extraction of salient surface loci (curvature extrema) of *tip-* and *saddle-like structures* such as the tips of the ventricular horns or the saddle points at the zygomatic bones (see Fig. 1(a),(b)).

2 Model Fitting with Quadrics for Landmark Extraction

Quadrics for Surface Modeling To represent 3D tip-like structures, we utilize bended and tapered half-ellipsoids, while for saddle-like structures we employ hyperboloids of one sheet (see Fig. 1(c),(d) for illustration and [1],[3] for details). Hence, our model is described by the parameter vector $\boldsymbol{p} = (a_1, a_2, a_3$ (half-axes of the quadric), δ, υ (bending strength and -angle), ρ_X, ρ_Y (tapering parameters), X, Y, Z (translation parameters), α, β, γ (Eulerian angles)).

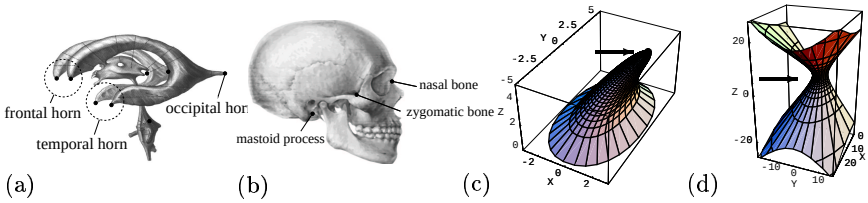

Abb. 1. (a),(b): Ventricular horns of the human brain and the skull. **(c),(d)**: Quadrics for modeling tips and saddle structures. Landmark positions are indicated by dots.

Edge-Based Fitting Measures for Model Fitting As an edge strength-based fitting measure, the gradient magnitude of the intensity function is integrated over the model surface, while for an edge distance-based fitting measure, the sum of first-order shortest distance approximations to the model surface is calculated over the image data (see [1] for details).

Hybrid Optimization Local optimization algorithms such as the conjugate gradient (cg-)algorithm (e.g., [3]) tend to run into local suboptima unless a good model initialization is provided. Therefore, global algorithms such as genetic algorithms (GAs) are frequently proposed (e.g., [2]), but often have inacceptably slow convergence rates. As a combination of both, we propose a novel hybrid optimization strategy. Similar to GAs, we consider a whole population of parameter vectors. However, our mutation strategy is more problem-specific: At the end of each cg-step, a line search has to be performed. Instead of taking only one local minimum, we here consider several of such local minima. This is motivated by experiments - not reported here - where local suboptima resulting from a line search procedure lead to the global optimum of the whole optimization problem for model fitting. Depending on the optimization problem at hand, either an in-depth-search with few population members or an in-breadth-search with many population members is more successful. We therefore dynamically adapt the population size to the problem complexity by increasing the population size each time a population member converges to a local minimum. Several parameters can be adapted to the specific optimization problem at hand as, e.g., the minimum and maximum population size and the criteria, when to discard population members with too bad objective function values. We tried to experimentally determine parameter values that are applicable to a broad class of optimization problems (see [1] for details).

3 Experimental Results for 3D Tomographic Images

Scope of Experiments Our hybrid optimization algorithm has been compared to purely local cg-optimization w.r.t. poorly initialized model parameters using

- different *types of image data*: 3D MR and CT images of the human head,
- different *types of landmarks*: frontal/occipital horns of the lateral ventricles, zygomatic bones as part of the skull, and
- different *fitting measures*: edge distance-based and edge strength-based.

Experimental Strategy For obtaining poor initial values for model fitting, the parameter values of an initial good fit are varied by adding Gaussian distributed random numbers. In order to determine the landmark localization error e, the landmark positions calculated from the fitted deformable models are compared to ground truth positions that were manually specified in the 3D images. In addition, we consider the root-mean-squared distance between edge points of the image and the model surface, e_{RMS}. This procedure is iterated sufficiently often (here: 100 times) with different, randomized model initializations.

General Results Common to all experiments is that the final value of the fitting measure is better by about 10-50% for hybrid optimization than for purely local cg-optimization. In most cases, the landmark localization and the model

fitting accuracy also improve significantly. Thus, hybrid optimization turns out to be superior to purely local cg-optimization at the expense of an increase in computational costs by a factor of 5-10 (30s–90s for local cg-optimization and 150s–900s for hybrid optimization on a SUN SPARC Ultra 2 with 300MHz CPU).

Results for the Ventricular Horns The tips of the frontal and occipital horns of the lateral ventricles are considered here. Typical examples of successful model fitting are shown in Fig. 2. As can be seen from the averaged quantitative results in Table 1, hybrid optimization is superior to purely local cg-optimization and yields in most cases better model fitting (e_{RMS}) and landmark localization (e) results (cf. also Figs. 2(a),(b)). Note that rather coarsely initialized model parameters have been used ($\overline{e}_{initial} \approx 7 \ldots 9\, vox$), and thus some unsuccessful fitting results – particularly in the case of the less pronounced occipital horns – deteriorate the average accuracy of model fitting as shown in Table 1.

Results for the Zygomatic Bones All results for the zygomatic bones were obtained with our edge strength-based fitting measure. Model fitting for the saddle points at the zygomatic bones (e.g., Fig. 2(c)) in general is not as successful as it is for the tips of the ventricular horns. However, the mean landmark localization error $\overline{e}$ can be reduced from initially $\overline{e}_{initial} = 6.4 \ldots 6.9\, vox$ to $\overline{e} = 2.5 \ldots 3.2\, vox$ and the accuracy of model fitting is $\overline{e}_{RMS} = 1.5 \ldots 1.8\, vox$ (voxel size $= 1.0\text{mm}^3$).

4 Conclusion

Experimental results demonstrate the applicability of our hybrid algorithm as well as its increased robustness for the case of poorly initialized model parameters as compared to a purely local cg-method.

References

1. Alker M, Frantz S, Rohr K, et al.: Improving the Robustness in Extracting 3D Point Landmarks from 3D Medical Images Using Parametric Deformable Models. Procs MICCAI 2001:582–590, 2001.
2. Delibasis K, Undrill PE: Anatomical object recognition using deformable geometric models. Image and Vision Computing 12(7):423–433, 1994.
3. Frantz S, Rohr K, Stiehl HS: Localization of 3D Anatomical Point Landmarks in 3D Tomographic Images Using Deformable Models. Procs MICCAI:492–501, 2000.
4. Rohr K: On 3D differential operators for detecting point landmarks. Image and Vision Computing 15(3):219–233, 1997.

		Model initi-alization	Edge dist.-b. fitt. meas.		Edge strength-b. fitt. meas.	
			local cg-opt.	hybrid opt.	local cg-opt.	hybrid opt.
Frontal horn (left)	$\overline{e}$	7.71 ± 3.16	3.28 ± 2.99	1.40 ± 1.18	3.54 ± 2.18	2.49 ± 2.21
	$\overline{e}_{RMS}$	2.22 ± 1.10	1.00 ± 0.63	0.65 ± 0.22	1.04 ± 0.31	0.87 ± 0.35
Frontal horn (right)	$\overline{e}$	6.57 ± 3.18	3.87 ± 2.16	3.15 ± 2.18	6.55 ± 3.53	5.19 ± 3.70
	$\overline{e}_{RMS}$	2.12 ± 1.11	1.05 ± 0.60	0.78 ± 0.25	1.56 ± 1.26	1.28 ± 0.79
Occipital horn (right)	$\overline{e}$	9.08 ± 4.42	6.90 ± 3.89	6.68 ± 3.93	4.74 ± 4.33	4.61 ± 4.31
	$\overline{e}_{RMS}$	3.00 ± 1.40	2.06 ± 0.93	2.04 ± 0.87	1.34 ± 0.87	1.29 ± 0.78

Tabelle 1. Fitting results averaged over 100 model fittings with randomized poor model initializations for 3D MR images of the *frontal/occipital* ventricular horns using *13 model parameters* ($\overline{e}$: mean landmark localization error (in *vox*), $\overline{e}_{RMS}$: RMS distance between deformable model and image data (in *vox*), voxel size $= 0.86 \times 0.86 \times 1.2\text{mm}^3$).

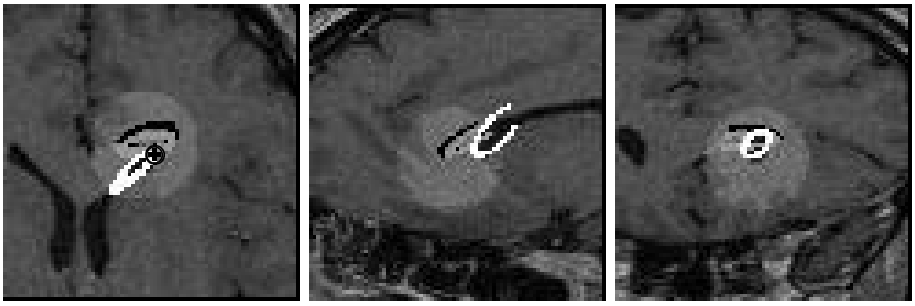

(a) 3D MR image of the *frontal* horn of the *left* lateral ventricle, edge *distance*-based fitting measure, ROI size 15.0 *vox*

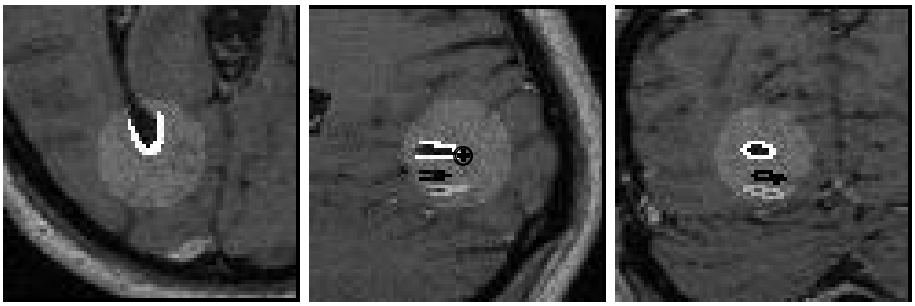

(b) 3D MR image of the *occipital* horn of the *right* lateral ventricle, edge *strength*-based fitting measure, ROI size 15.0 *vox*

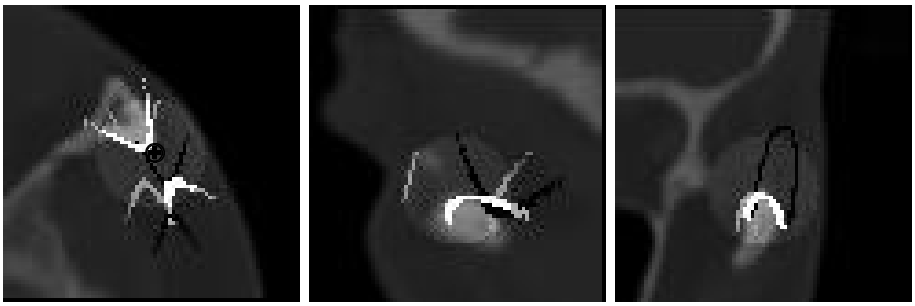

(c) 3D CT image of the *left* zygomatic bone, edge *strength*-based fitting measure, ROI size 15.0 *vox*

Abb. 2. Examples of successfully fitting tapered and bended half-ellipsoids to 3D MR images of the frontal and occipital horns of the lateral ventricles (Fig. 2(a-b)) as well as of fitting a half-hyperboloid with no further deformations to a 3D CT image of the zygomatic bone (Fig. 2(c)). Contours of the model surfaces in axial, sagittal, and coronal planes are depicted here (from left to right). *Black*: model initialization, *grey*: fitting result for local cg-optimization, and *white*: fitting result for our hybrid optimization algorithm. The ground truth landmark positions are indicated by a $\oplus$-sign.